ANNIVERSARY REVIEW

Wood—a 45th anniversary review of JMS papers. Part 1: The wood cell wall and mechanical properties

Martin P. Ansell

Abstract The first part of a comprehensive review of the literature on wood published in the Journal of Materials Science since its inception in 1966 is presented. Papers are reviewed by subject ranging from the determination of the microfibril angle in the wood cell wall through to the evaluation of fatigue life. The role of moisture content in determining mechanical properties of wood is explored and mechanical properties are reported including creep, fatigue and fracture. It is concluded that JMS has played a key role in disseminating state of the art literature on new developments in the understanding of the structure-related properties of wood.

Introduction

The Journal of Materials Science (JMS) has made a significant contribution to the publication of papers on wood since the first volume was published in 1966. As a Materials Science undergraduate at the University of Sussex from 1968 to 1971, the author is proud to have been taught by the late Professor Robert Cahn, the inaugural editor of JMS, and to have consulted the journal to support project work in his final year. Many years later, after an academic career in materials science with a major interest in the science and engineering of wood, it is a pleasure to review progress in wood science published within the pages of JMS. The earliest papers reviewed here date from 1977 but since then wood-related output has steadily grown.

M. P. Ansell (✉)
BRE Centre for Innovative Construction Materials,
Department of Mechanical Engineering, University of Bath,
Bath, BA2 7AY, UK
e-mail: M.P.Ansell@bath.ac.uk

Research on wood and timber is truly international, reflecting the universal role that wood plays in all our lives, mainly in construction but also in furniture, transport, sport, musical instruments and many other applications. In the UK, the Building Research Establishment's Forest Products Research Laboratory (FPRL) was created at Princes Risborough Laboratory in 1927 and key progress was made in measuring the mechanical properties of wood, advancing timber utilisation and combating degradation from fungal decay and insect attack. In the 1960s, the introduction of electron microscopy allowed microstructure to be linked to properties and the wood composites industry explored the development of new wood products such as medium density fibreboard. Well established degree programmes in wood science at the Universities of Aberdeen and Bangor prepared students for careers worldwide.

Sadly, UK degree programmes in wood science no longer exist and FPRL was absorbed onto BRE's Garston site in 1988. However, timber trading is still a significant factor in the UK economy. The latest national statistics on UK Wood Production and Trade produced by the Forestry Commission (May 2011) state that in 2010 the UK imported 5.7 million m^3 of sawn wood, 2.7 million m^3 of wood-based panels and 8.0 million tonnes of pulp and paper with a total value of wood product imports of £6.7 billion balanced by £1.8 billion of exports (www.forestry.gov.uk/forestry). Approximately 0.25 million employees in the UK rely on wood as a source of income. Despite the high profile of wood, a major UK research council has recently stated that 'research investment in the timber and wood industries is not a major priority'.

Nevertheless, attention worldwide continues to focus on fundamental and applied aspects of wood science and JMS continues to publish an increasing number of papers in these fields. The literature on the science of wood is

immense and notable journals devoted principally to wood include Wood Science and Technology, Holzforschung, Wood and Fiber Science, Journal of Wood Science, International Wood Products Journal (formerly Journal of the Institute of Wood Science) and Wood Material Science and Engineering. The JMS papers, reviewed below, reflect the work of research groups from Japan, China and Australasia through to Europe and North America. The review is split into sections by subject area including the micromechanics of the wood cell wall, moisture-related properties of wood, mechanical properties, creep, stress relaxation, fracture and fatigue. In the second part of the review, wood modification, thermal properties and fire, carbonised wood and chars and finally wood–polymer and wood–cement composites will be included. With a view to restricting the review to a manageable size, the majority of papers reviewed here were published in JMS and other literature sources are only cross referenced for the sake of clarity. References cited in the reviewed papers provide links to the broader literature.

Measurement of the microfibril angle in the wood cell wall

Understanding the relationship between the orientation of cellulose microfibrils in the wood cell wall and the mechanical properties of wood has been a preoccupation of wood scientists for many years. Key textbooks which describe the cell wall nanostructure, microstructure and engineering properties of wood include Dinwoodie [1] and Bodig and Jayne [2]. The primary (P) and secondary (S1, S2 and S3) cell walls contain bundles of cellulose molecules, known as microfibrils, within a matrix of lignin, hemicelluloses, pectins, waxes and extractives. The structural features of the wood cell wall are depicted in Fig. 1 [3] together with a depiction of the ultrastructural organisation of cellulose, hemicellulose and lignin in the cell wall. The S2 layer is the thickest and the microfibrils are
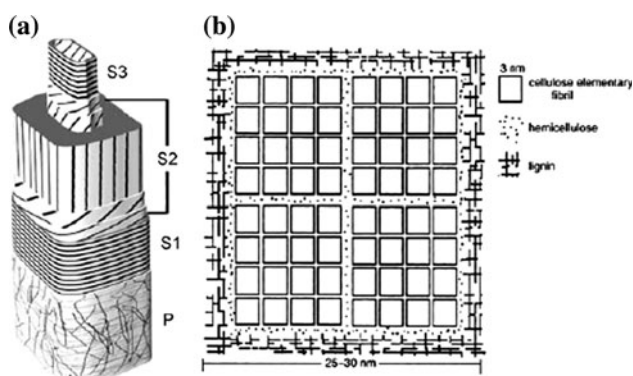
Fig. 1 a Schematic design of wood cell wall of a softwood fibre. b Ultrastructural organisation of cellulose, hemicellulose and lignin [3]

oriented in a right hand spiral (Z helix) with an inclination to the major cell axis known as the microfibril angle (MFA). Smaller MFAs result in higher stiffness (Young's modulus) measured along the cell axis. There are variations in MFA across annual rings in temperate woods with earlywood (lower density cells laid down at the beginning of the growth season in temperate climates) tending to have higher MFAs than latewood (higher density cells laid down at the end of the growth season). Earlywood and latewood are organised in concentric annual rings with the youngest wood nearest the bark of the tree. The first 10–20 annual rings are known as juvenile wood and the MFA is consistently higher than in mature wood outside this zone. Wood therefore has a hierarchical structure building up from the disposition of cellulose microfibrils in a predominantly hemicellulose and lignin matrix, through to the multi-layer cell wall and then to the arrangement of concentric earlywood and latewood zones.

Entwistle and co-workers [4–7] used small angle X-ray scattering (SAXS) to determine MFA in softwoods, mainly *Pinus radiata*. At the boundary of adjacent cells, the cellulose microfibrils in the S2 layers contra-spiral in an idealised structure. By directing the X-ray beam at 45° to both sets of cell walls, the S2 MFA can be deduced from the average azimuth angle obtained from merged X-ray intensity maxima at the (002) diffraction circle [4]. Subsequent papers evaluated variations in the actual structure of cellular arrays in wood to determine possible errors from assuming an idealised structure [5] and assuming that cell walls were either in the tangential or radial orientations [6]. Only a few degrees of error in measuring the MFA in the range from 20° to 30° were predicted using the SAXS method. A thousand cell walls in *P. radiata* were examined by image analysis and MFAs were determined from the (002) diffraction intensities at different angles of X-ray incidence [7]. It was concluded that a model based on square section wood cells is adequate for the prediction of MFA and that an X-ray incident angle of 45° is optimum. SAXS was also employed by Färber et al. [8] to evaluate variations in MFA across a branch of Norway spruce (*Picea abies*). In compression wood the MFA decreased progressively from the tree trunk to the branch tip but there were large variations in MFA depending on the age of the branch. It should be noted that other methods for the measuring MFA in the S2 layer include X-ray diffraction, polarized light microscopy, confocal microscopy, iodine precipitation, inducement of cracking by UV radiation, measurement of pit aperture angles and the application of soft rot fungi to reveal the orientation of microfibrils [9]. Commercial SilviScan™ equipment was developed in the 1990s at CSIRO, Australia which measures wood density using an X-ray densitometer and MFA with an X-ray diffractometer (http://csiropedia.csiro.au/).

Investigation of the wood cell wall

Jang et al. [10] produced images of cross-sections through individual unbleached softwood Kraft pulp wood fibres using confocal laser scanning microscopy, avoiding the need to section the fibres with a microtome. Optical sectioning in the epifluorescent mode combined with image analysis allowed accurate estimation of the cross-sectional area and the thickness of the cell wall. Atomic force microscopy (AFM) in conjunction with image processing of spruce (*Picea* sp.) wood, before and after processing into Kraft pulp fibres, allowed the disposition and size of cellulose aggregates in the secondary cell wall [11] to be determined. AFM was also used by Navaranjan et al. [12] to evaluate the flexural properties of single pulp wood fibres of *P. radiata* in a three point bend test confirming the stiffer behaviour of latewood fibres.

The dependence of the mode of fracture and ductility of the wood cell wall on MFA was assessed by Reiterer et al. [13] using SAXS and scanning electron microscopy (SEM) and a large microfibril angle resulted in less brittle failure and higher extensibility (longitudinally and transversely) and toughness. Bergander and Salmén [14] examined the roles of cellulose, hemicellulose and lignin in determining the longitudinal and transverse properties of the wood cell wall, emphasising the contribution of the S1 and S3 layers as well as the dominant S2 layer. In an investigation of the acoustic properties of softwoods for violin and piano soundboards, Hori et al. [15] employed X-ray diffraction to measure crystal width and MFA of earlywood (EW) and latewood (LW) in several spruce species and measured the specific Young's modulus (E/ρ) and loss tangent (tan δ) in acoustic tests. E/ρ was found to have a strong negative correlation with MFA in EW and LW. A high crystal width is associated with high E/ρ and low damping. Sitka spruce (*Picea sitchensis*) was identified as having an especially low MFA, which is similar in both EW and LW, and these characteristics confirm its reputation as the best soundboard material.

Sometimes a paper appears that is especially striking in its elegance and impact. The in situ bending technique described by Orso et al. [16] to measure the cell wall properties of spruce is such a paper, submitted and accepted for publication by JMS in the space of 12 days. A focussed ion beam (FIB) in a SEM was used to machine tiny cantilever beams from the wood cell wall, approximately 20 µm wide and 3.5 µm thick. A piezoresistive AFM tip mounted on a three-axis micro-manipulator applied force to the end of the cantilever (Fig. 2) enabling the elastic modulus of the cell wall material to be measured on loading (av. 29.9 GPa) and unloading (av. 26 GPa). A tendency for the cantilever to twist following FIB
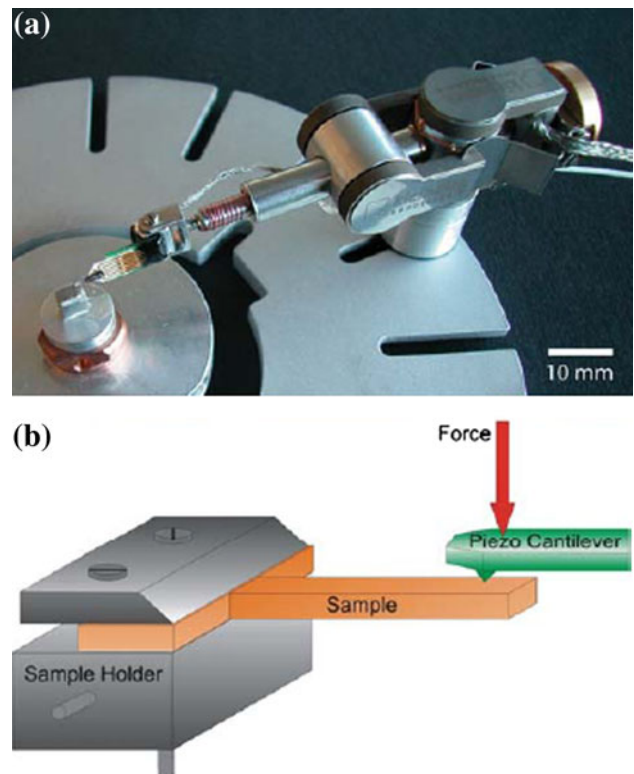
Fig. 2 **a** Testing device, **b** schematic of the bending test for cantilever section of the wood cell wall [16]

machining is likely to relate to the MFA of the cellulose microfibrils in the S2 cell wall.

Nanoindentation has been employed to evaluate variability in the mechanical properties of the wood cell wall. Konnerth et al. [17] investigated variation in hardness as a function of MFA, specimen and fibre orientation, shape of indenter tip and method of specimen preparation. The geometry of the indenter (pyramid or cone) affected hardness results and the correct alignment of the indenter with the fibre axis was crucial as determined by confocal Raman spectroscopy. The hardness of softwood (Scots pine, *Pinus sylvestris*) and hardwood (*Eucalyptus* sp.) pulp fibres was also assessed by nanoindentation [18] in order to assess the effect of bleaching on mechanical properties. Bleaching reduced the indentation hardness of softwood pulps but slightly increased the hardness of hardwood pulps. Tomographic slice images were used by Xu et al. [19] to evaluate the variability in the orientation of high angle S2 microfibrils in thin strips of *P. radiata* containing compression wood. The average values of strength and stiffness were low with large variations due to kinks in microfibrils and the dislocation of microfibrils into segments.

It should be noted that microfibrils can be mechanically or chemically broken down into their nano-fibrillar constituents and the current literature on micro-fibrillated

cellulose and nano-cellulose is very extensive. See, for example the paper by Bulota et al. [20] on the reinforcement of poly(vinyl) alcohol reinforced with mechanically micro-fibrillated birch Kraft pulp.

Moisture, creep and stress relaxation

The relationship between moisture bound in the wood cell wall and mechanical properties is well known and the properties of wood are quoted in relation to moisture content measured as a proportion of dry weight. In general, strength and stiffness increase with decreasing moisture content and, in tension, any non-linear behaviour at strains close to the peak stress is reduced. The proportion of bound moisture in the wood cell walls strongly influences deformation as a function of time in the form of creep (at constant stress) and stress relaxation (at constant strain). A further type of deformation, termed mechano-sorptive behaviour, occurs when stressed or strained wood experiences changes in moisture content during its loading history. Drying (desorption) and wetting (adsorption or sorption) of wood during creep or stress relaxation can have a profound effect on accelerating deformation in comparison to behaviour at constant moisture content. Further background information on wood–moisture relationships is provided by Dinwoodie [1]. The complexity of moisture–mechanical properties relationships in wood and the breadth of the literature are such that JMS papers in this field are reviewed chronologically.

Creep

A long-term evaluation of creep in chipboard and other panel products was initiated at FPRL's Princes Risborough site and eventually moved to Garston. The first of an extensive series of papers on creep of chipboard [21] was concerned with fitting three and four element visco-elastic–plastic models to the creep data. Papers by Hunt at South Bank Polytechnic evaluated creep in wood under conditions of concurrently changing humidity. In work on beech (*Fagus sylvatica*) in tension, a threshold compliance was determined [22] below which sorption or desorption increased the rate of creep. A new creep machine which operated in bending was described in a second paper [23] where for two pine species mechano-sorptive creep was directly influenced by the MFA and correlated with the elastic compliance of the wood. Corrections for density and dimensional changes resulted in the concept of a reduced creep (time-dependent) compliance whereby the making and breaking of hydrogen bonds are triggered by changes in humidity and moisture content. In a later paper, axial dimension changes in unloaded softwood specimens were

measured in response to changes in moisture content. The idea of two energy levels for moisture bonding were proposed [24], with a high energy moisture being associated with dimensional changes with little hysteresis (Fickian diffusion) and a lower energy moisture associated with hysteresis only (non-Fickian). Hunt also reports on the modification of tensile creep apparatus for work on compressive creep [25]. After moisture cycling and load reduction, a stable mechano-sorptive creep limit was reached. Thereafter, creep and creep recovery were observed to be in balance. Variations in the longitudinal moisture-swelling coefficient were a result of the strain being less in tension and greater in compression. Entwistle and Zadoroshnyj [26] applied shear stresses in torsion to Radiata pine (*P. radiata*) specimens under conditions of cyclic humidity. Mechano-sorptive strains developed which far exceeded the initial elastic strain. In view of the little change in shear modulus observed, it was concluded that the breaking and remaking of hydrogen bonds between parallel molecular chains was responsible for the high shear strains in agreement with Hunt [23].

Stress relaxation

Relaxation behaviour in wood has been reported by a number of authors including Kelley et al. [27] who used dynamic mechanical analysis (DMA) and differential scanning calorimetry to identify glass transitions (T_g) associated with amorphous components (lignin and hemicellulose) in the wood cell wall. Changes in moisture content shifted values of T_g, modelled by the Williams-Landel-Ferry relationship, and it was concluded that the amorphous components of the cell wall are immiscible and behave independently. Kubat and co-workers investigated stress relaxation in Scots pine wood (*P. sylvestris*) [28, 29] as a function of stress and humidity and modelled relaxation with a collaborative flow model with two stages of relaxation. Ebrahimzadeh and Kubat [30] reported that step-wise humidity changes applied to Scots pine wood resulted in changes in damping and stress relaxation rates that were accelerated by these changes. In a later paper [31], the dynamic mechanical response of Scots pine was analysed using coupled non-linear rate equations as a function of time and two water molecule binding modes were proposed to model the sorption and desorption of water. Eligon et al. [32] examined adsorption and desorption of ten species of tropical hardwoods exposed to conditions of cyclic relative humidity, noting changes in dimensions and moisture content. Hysteresis was observed in both these variables as a function of relative humidity with an anomalous contraction observed below 2% moisture content. Wadso [33] specified four conditions for the sorption of water into wood cell walls by non-Fickian

diffusion and observed that there was no suitable model available to predict diffusion behaviour. Furuta et al. [34] conditioned Japanese hinoki (*Chamaecyparis obtusa*) to various moisture contents between 0 and 150 °C and observed a relaxation at around 40 °C and deduced that this relaxation was due to the cellulose and hemicellulose by comparison with the behaviour of solutions of these polysaccharides. Stress relaxation experiments were performed on Japanese oak (*Quercus* sp.) by Nakao and Nakano [3] and a Kohlrausch–Williams–Watts function was used to model the response as a function of moisture content.

A comprehensive model of the wood cell wall was constructed by Neagu and Gamstedt [35] to determine hygroelastic properties as a function of loading and changes in moisture content. Twisting was the dominant factor found to influence expansion following increase in moisture content. The plasticisation of wood following saturation by water up to 135 °C was examined by Placet et al. [36] using DMA based on the flexure of a single cantilever beams of oak (*Quercus sessiliflora*), beech (*F. sylvatica*), spruce (*P. abies*) and fir (*Abies pectinata*). A glass transition at between 70 and 105 °C was ascribed to saturated lignins but some thermal degradation of properties was observed during the experiments. The results of the work can be related to the drying of green wood. Arnold [37] examined the effect of moisture on the bending properties of beech (*F. sylvatica*) and spruce (*P. abies*) following thermal modification (reviewed in Part 2 of this paper). In general the bending performance of modified wood is less affected by moisture content but the mechanical behaviour is more brittle.

Overall, a picture emerges of wood as a moisture-sensitive, cellular, organic material where the uptake and loss of moisture facilitates creep and stress relaxation and resulting deformation is controlled by the orientation of cellulose microfibrils in the primary and secondary cell walls.

Mechanical properties

The literature on the mechanical properties of commercial wood species is widespread and two classic sources are Lavers [38] on the strength properties of timber and the Wood Handbook [39] originally published by the US Department of Agriculture. The strength properties of sawn and dried wood in the form of timber are divided into grades and strength classes outside the scope of this JMS review but for general interest, design with timber is embodied in Eurocode 5 [40]. Wood properties are highly anisotropic and dependent on moisture content and less so on temperature and rate of loading. JMS has included a fairly limited number of papers in this field.

Kahle and Woodhouse [41] were inspired to model the microstructure of wood as a honeycomb by the desire to determine the ideal properties of Norway spruce (*P. abies*) for the soundboards of musical instruments. The twelve elastic constants required to characterise the elastic properties of wood were reduced to nine via a reciprocal relationship that reduced the number of independent Poisson's ratios from six to three. Wood structure was modelled as a honeycomb with reference to 500–700 cells in four specimens of spruce. A good correlation between the modelled properties of the honeycomb with the measured elastic properties of spruce was achieved and the refinement in modelling the wood cell wall was proposed to improve the predictions. Spruce wood for soundboards was also the topic of a paper by Obataya et al. [42]. Elastic constants for Sitka spruce (*P. sitchensis*) specimens were measured, including the dynamic Young's modulus and loss tangent along the grain, the dynamic shear modulus, the loss tangent in the vertical section and density, by free–free flexural vibration and torsional vibration (Fig. 3). A relative acoustic conversion efficiency and a ratio reflecting the wood anisotropy were proposed for assessing soundboard quality. From a simple model of the wood cell wall it was concluded that small MFAs produced superior soundboards.

A paper by Eichhorn et al. [43] on the applications of Raman spectroscopy for understanding deformation mechanisms in cellulosic materials included tensile testing of sections of *P. radiata* wood with a S2 MFA of 13°. Wood was sectioned into small slivers and glued onto PMMA beams for loading in four-point bending. A Raman spectrum was captured at intervals of strain with the laser beam polarised parallel to the cell wall. The 1095 cm^{-1} Raman peak (Fig. 4a) associated with cellulose shifted to lower wavenumbers during tensile straining (Fig. 4b). The scatter
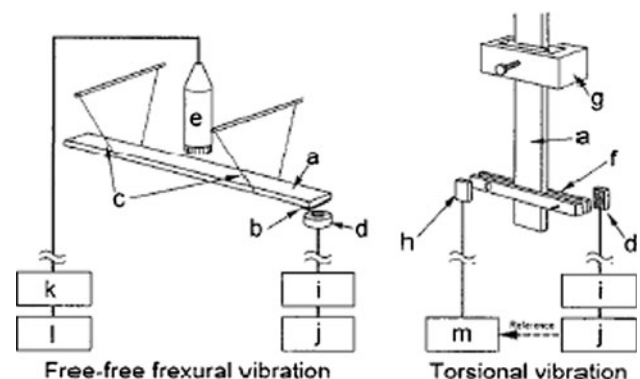
Fig. 3 Schematic diagrams of free–free flexural vibration apparatus and the torsional vibration apparatus. (*a*) wood specimen, (*b*) iron piece, (*c*) silk thread supporting the specimen, (*d*) magnetic driver, (*e*) microphone, (*f*) iron weight, (*g*) clamp, (*h*) detector, (*i*) amplifier, (*j*) generator, (*k*) band-pass filter, (*l*) FFT analyzer, (*m*) lock in amplifier [42]
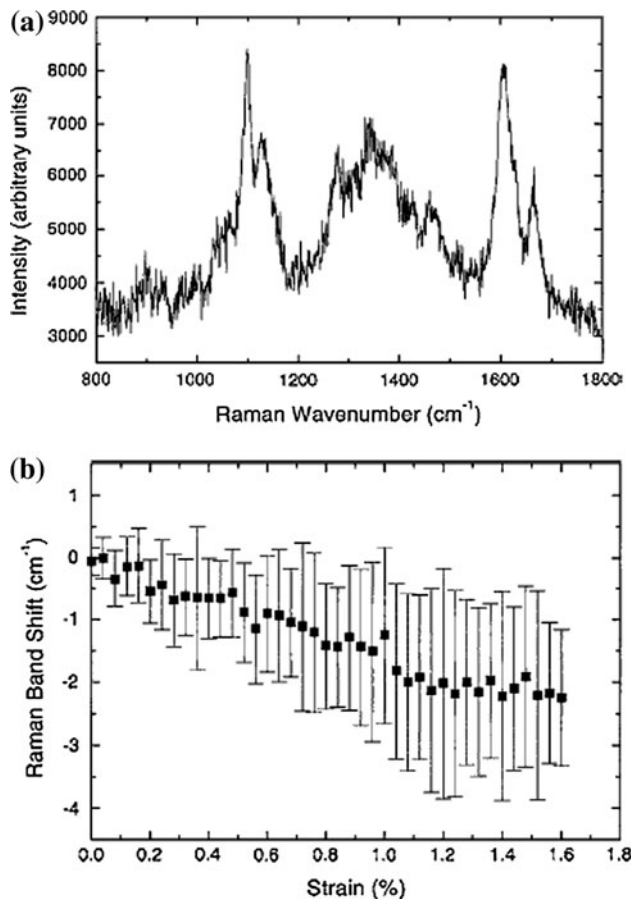
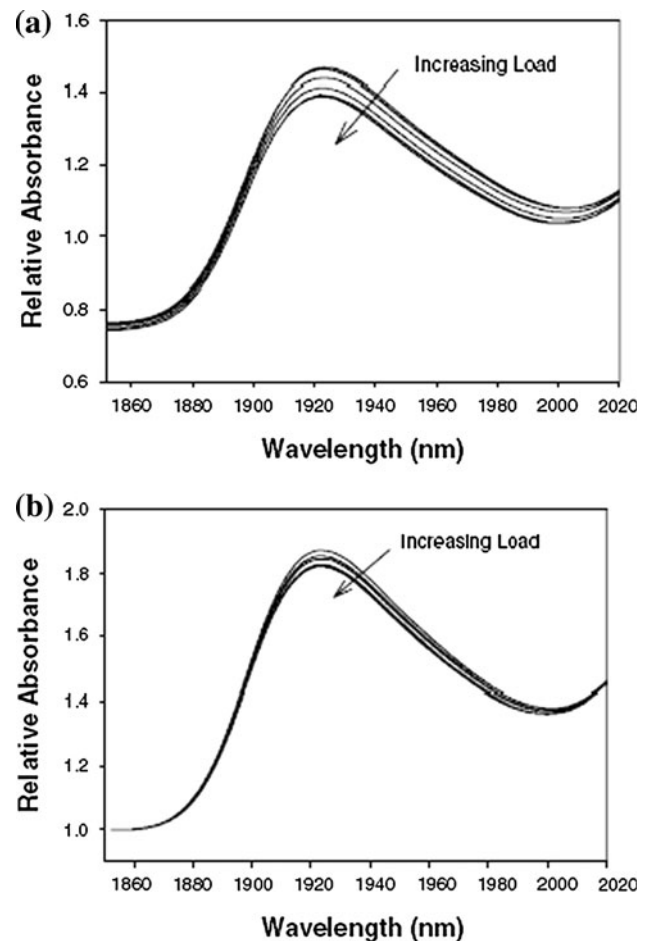Fig. 4 **a** Raman spectrum of *P. radiata* wood, **b** the variation of Raman band shift with tensile strain obtained from four-point bend tests for seven different *P. radiata* samples [43]

Fig. 5 Effect of increasing load on the NIR spectra (1850–2020 nm) taken from the **a** tension face and **b** compression face of yellow poplar beams [44]

observed results from the difficulty in focussing on the S1, S2 or S3 secondary wall layer. No shift occurred in the 1600 cm^{-1} band which was associated with lignin. Hence the lignin appears to be transferring very little load which is carried principally by the cellulose microfibrils.

André et al. [44] used an alternative technique for measuring strain in stressed wood using near infrared (NIR) spectroscopy. Shifts in NIR absorption spectra as a function of load in the wavelength range from 1850 to 2020 nm (Fig. 5) enabled the loads on the tension and compression faces of yellow poplar stressed in four-point bending to be predicted. These spectra were compared using principal component analysis and it was concluded that the chemical groups that are moving under applied load in tension and compression are different. Essentially, the cellulose microfibrils are more likely to respond to tension whilst the hemicellulose and lignin are dominant in compression.

The anisotropy of wood was examined by DMA in a paper by Backman and Lindberg [45] who examined the dynamic properties of *P. sylvestris* in the radial and tangential directions. Clear sapwood specimens were 3 mm wide by 1.3 mm thick (Fig. 6a) and experiments were conducted in the temperature range from −120 to 80 °C in tension. The radial storage modulus was greater than the tangential value across the whole temperature range (Fig. 6b), corresponding with static mechanical properties. This difference was initially postulated to be due to the presence of ray cells and off axis cellulose microfibrils at pit openings but is more likely to be the result of the low tangential stiffness of earlywood. There were also differences in the α, β and γ peaks in the tan δ versus temperature characteristics for radial and tangential material with an α peak at 0 °C observed in the tangential direction. The thermo-mechanical properties of wood, fibreboard and laminated wood were also investigated with DMA [46] in the temperature range −100 to 150 °C. A low temperature thermal transition was observed at −50 °C associated with bound water (chemically bonded in the wood cell wall) and higher temperature thermal softening occurred between 40 to 120 °C.

Fig. 6 a DMTA samples for tensile testing for the (a) radial and (b) tangential directions, b dynamic elastic modulus versus temperature for the radial and tangential directions. *Error bars* indicate 95% significance in a one-sample *t* test [45]
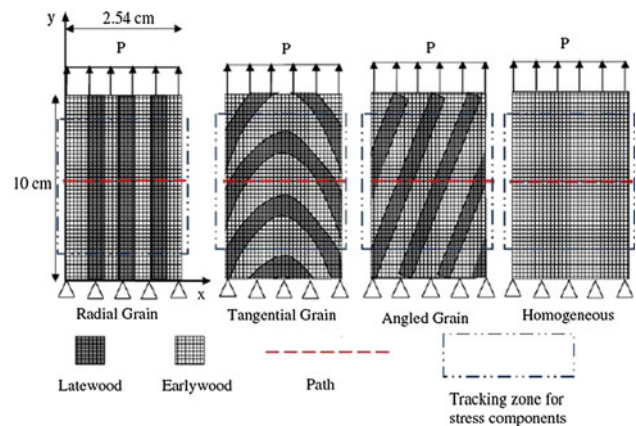
modes influence the apparent moduli of the two wood species. In compression shear, the axial stiffness of the cypress increased but the stiffness of the beech was unchanged.

In a thought-provoking paper on the anisotropic properties of wood, Katz et al. [48] compared the elastic properties of softwoods and hardwoods with those of bone on the basis they possess similar hierarchical structures. Ultrasonic wave propagation measurements on bone were extended to those for softwoods and hardwoods enabling the elastic moduli (Cij) and Poisson's ratios for wood to be calculated. Scalar anisotropy factors for shear and compression were also computed and values for the elastic constants of cellulose, hemicellulose and lignin were derived.

The dependence of yield in softwoods on strain rate and moisture content were evaluated [49] by measuring the crushing strength of *P. radiata* and *Kahikatea*. A flow stress equation was developed based on the assumption that the thermally activated motion of microfibrils over short range barriers and the activation volume are both a function of moisture content.

Finite element methods were employed [50] to predict the ultimate tensile stress (UTS) of wood strands based on radial grain, tangential grain, angled grain and homogenous structural analogues (Fig. 7). A deterministic method (FEM) and a stochastic method (SFEM) were used to assess the effect of grain orientation and earlywood and latewood properties on the UTS of wood. Cumulative probability distributions for UTS as a function of growth ring orientation were computed for the four structural analogues using FEM and SFEM and they corresponded well with experimental results for loblolly pine with no significant difference. The same authors also published work [51] on the application of differential image correlation to evaluate the orthotropic elastic properties of loblolly pine (*Pinus taeda*) [37]. The orientation of pine wood

Japanese beech (*Fagus sp.*) and cypress (*C. obtusa*) wood were subjected to combined axial stress (along the longitudinal axis) and torsional stress (about the longitudinal axis) [47]. A proportional deformation loading method and an initial constant loading method were used. In the former method the axial displacement rate and the rate of torsional rotation were kept constant and the ratio was varied. In the latter method axial force or torque was applied as a pre-load and torque or axial force, respectively, was then applied at a constant rate. Dimensionless failure loci under axial-shear combined stress were generated for each loading method and the apparent shear modulus and apparent Young's modulus were obtained as a function of the angular rotation. The different loading

Fig. 7 Structural analogue of strand orientation models [46]

strands again made a significant difference to the properties measured.

JMS papers have therefore showcased a wide range of mechanical and vibrational techniques for measuring the mechanical properties of wood at micro- and macroscopic levels. In recent years, new spectroscopic (e.g. Raman) and modelling techniques (e.g. FEM) have been introduced for measuring and predicting the fundamental elastic constants and mechanical behaviour of wood.

Fracture of wood

The design stress that may be applied to wood in timber structures depends on the time under load or duration of load (DOL). As the projected DOL increases, the design loads must be reduced. The effect of rate of loading and DOL on the strength of Douglas fir (*Pseudotsuga menziesii*) timber were considered by Nadeau et al. [52]. Time-dependent, delayed fracture effects were explained by the kinetics of sub-critical crack growth based on the application of fracture mechanics. The fracture model offered a probabilistic approach to timber design. In an influential paper relating wood microstructure to the micro-mechanical behaviour of wood, Boatright and Garrett [53] employed a general fracture mechanics approach to improve the understanding of toughness, fatigue and crack propagation in wood. They related the geometry of the cellular structure of wood, specimen thickness and the strain at crack tips to the process of crack tunnelling and ultimate fracture. At the crack tip, deformation involves debonding between cells and twisting and buckling of cells. A strain-based criterion for the fracture of pre-notched wood specimens was proposed based on a linear relationship between notch root radius and crack opening displacement. Experiments were undertaken within an SEM to observe fracture along the grain in micro-balsa (*Ochroma pyramidale*) wood compact tension (CT) specimens [54]. Balsa is a tropical hardwood with no annual rings and especially low density and is a model material for fracture studies in wood. A wedge was slowly driven into the CT notch to enable the mode of crack propagation to be observed. The surface of the fracture plane was far from flat and splitting within the cell walls and fracture perpendicular to cell walls were observed.

A non-destructive evaluation of damage caused by four-point flexural loading of Douglas fir (*P. menziesii*), red (*Q. rubra*) and pendunculate (*Q. robur*) oak and beech (*F. sylvatica*) was conducted by Vautrin and Harris [55]. The top and bottom faces of the beams were in the radial-longitudinal orientation. Some Douglas fir beams were also cut in the tangential-longitudinal orientation. Normal and reaction wood were investigated using the ring-down

acoustic emission (AE) technique where AE counts are recorded above a pre-set threshold. The higher density oak specimens generated high AE rates, typical of fast, brittle failure events, and AE output was generally species dependent.

In two papers, Prokopski [56, 57] applied fracture mechanics to the mechanical testing of wood. In the first paper, mode I tests were performed on pine (*Pinus* sp.), alder (*Alnus* sp.) and birch (*Fagus* sp.) to measure the critical stress intensity factor K_{IC} and results were found to be highly orientation-dependent. Tests were also performed in tension, compression and flexure but there was little correspondence with the K_{IC} results. In the second paper, the mode II (shear) critical stress intensity factor K_{IIC} was measured with the shear crack running in the three major longitudinal, transverse and radial directions (Fig. 8a). The test configuration is depicted in Fig. 8b. Birch wood was approximately 50% tougher in shear than the pine and alder, reflected by the mode of fracture imaged in the SEM.

Thuvander et al. [58] published a series of three papers on wood fracture in a single issue of JMS. In the first paper [58], finite element analysis was used to model the way in which the stiffness of wood varies from one annual ring to the next in a repetitive fashion. Three radial zones of a growth ring were defined, namely earlywood, transition wood and latewood (Fig. 9). The tangential-radial (TR) crack plane is depicted in Fig. 9 with the crack propagating
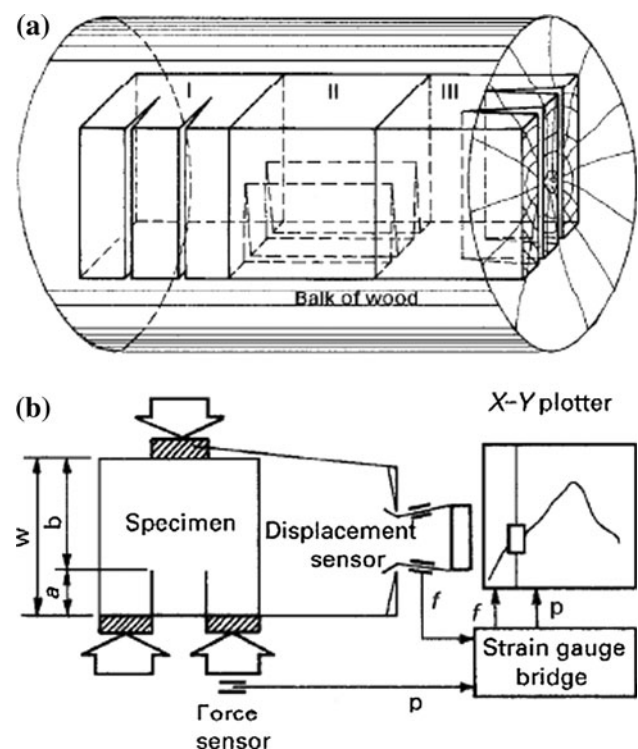
Fig. 8 a Orientation of mode II fracture specimens [57]. b Mode II fracture mechanics test [57]
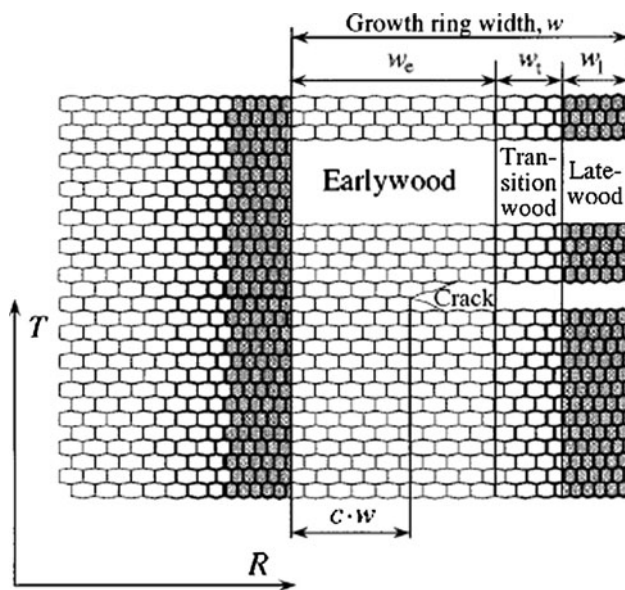
Fig. 9 The radial zones of a growth ring [58]

in the radial direction parallel to the plane normal to the tangential axis. Stress concentrations at the tip of a transverse crack in a CT specimen were modelled and the influence of crack tip position, crack inclination and growth ring width on stress distributions was assessed. It was concluded that the latewood presents a barrier to crack propagation ahead of the crack tip in the earlywood. Wide growth rings will tend to cause deviations in the crack path but there will be a tendency for oblique cracks to align into the TR plane. In the second paper [59], the crack tip strain field was considered at the growth ring level using electronic speckle photography. Once again a TR crack was considered. In the lower density, softwood significant strain distributions were observed to extend in a tangential direction whereas in the high density latewood there is much more constraint and good correlation with an FE model was found. In the third paper [60], fracture tests were performed on *P. sylvestris* CT specimens in the TR plane. The results of physical testing corresponded well with FE predictions for crack arrest at latewood boundaries, the alignment of oblique cracks in the TR plane, the influence of annual ring width on crack propagation and the fracture mode of wood cells. Overall the three papers make an elegant contribution to the study of fracture in softwood.

A group of three papers by Reiterer and co-workers examined the fracture energy of spruce wood, the radial reinforcement of the structure of wood and the influence of moisture content on mode I fracture. Mixed mode I and II fracture was examined in the first paper [61] for crack propagation along the grain (RL and LR orientations) using a wedge splitting technique. An asymmetric wedge was employed to develop mixed mode loading and fracture

energies for mixed mode tests with a range of wedge angles were calculated with a higher mode II component with increasing wedge angle. Strength parameters were also used to reflect crack initiation in the two orientations. The ratio of RL to LR strengths was in the ratio 1:2 and a larger component of mode II fracture increased strength. The role of ray cells in determining the strength and fracture modes of wood was examined in a second paper [62]. Once again the RL and LR orientations of wood species were investigated by wedge splitting. Radial and tangential tensile strengths of ash (*Fraxinus excelsior*) and oak (*Quercus* sp.) were measured and rays were found to act as reinforcement in the RL crack propagation system. The rays are envisaged as acting as stiff pins which limit the shear between zones of less stiff earlywood and stiffer latewood. The effect of moisture content (MC) on mode I fracture of spruce wood (*P. abies*) was examined in the third paper [63] using the wedge splitting technique to measure specific fracture energy and the mode I critical stress intensity factor K_{IC}. Increased MC raised the ductility and increased the specific fracture energy of the spruce but as the MC increased from 7%, K_{IC} fell by about 20% and retained this lower value up to 55% MC, well above the fibre saturation point. The three previous papers represent a valuable introduction to fracture in softwoods with emphasis on the influence of microstructure and moisture content on crack propagation modes. It is well known that wood is very resistant to transverse fracture across the grain and fracture paths will deviate into easy propagation modes resulting in the splintery fracture commonly observed in wood.

The JMS papers on wood fracture are completed by a further set of three papers by Chen et al. on the fracture of wood in torsion. A thermal imaging technique was employed to observe crack nucleation and propagation in cylindrical samples of Scots pine (*P. sylvestris*) wood loaded in torsion [64]. Fracture occurred along the grain in the earlywood during static tests and the fracture path depended on the orientation of the grain to the sample axis. Stages of crack nucleation and growth were examined by thermal imaging and earlywood was observed to dissipate more thermal energy than latewood. It was possible to predict the locations of damage initiation under cyclic loading in torsion by observation of hot spots. Acoustic emission (AE) was also employed as a tool for assessing damage development in softwood and hardwood samples under torsional loading in static and cyclic tests [65]. Ringdown counting were recorded above a threshold and related to damage development and fracture. As the grain angle increased from 0° to 45°, the AE counts decreased but then increased from 45° to 90°. A third paper [66] was concerned with fracture of red lauan (*Shorea teysmanniana*) (hardwood) and Sitka spruce (*P. sitchensis*) (softwood) in torsion. As well as relating fracture topography to

specimen orientation in static tests, some long-term fatigue tests were performed (displacement controlled) where changes in the slope and area of hysteresis loops were monitored. Fracture was a combination of modes I, II and III depending on the specimen orientation. The pattern of damage development, reflected in changes in the shape of hysteresis loops, was quite complex with significant differences between the hardwood and softwood specimens.

Fatigue properties of laminated wood

In the mid-1980s, the European wind turbine industry was engaged in the development of prototype wind turbines based on horizontal axis and vertical axis technology. The rapid expansion in US wind farms, driven by tax incentives, had resulted in the manufacture of a plethora of fibre-reinforced plastic (FRP) blades of variable quality which frequently suffered from delamination and failure at the hub connection. Attention transferred to laminated wood technology, based on thick veneers (3–4 mm), which could be laid up in moulds allowing quite tight curvatures to be achieved for aerofoil blade design. Furthermore, studs for attachment to the hub could be bonded directly into the laminated wood. The example of the Gougeon Brothers [67] in the design of laminated wood yachts was translated to the design of horizontal axis turbine blades in both the US and the UK.

Fundamental data on the fatigue life of wood under constant amplitude and complex loads was not available in the literature so Ansell and co-workers at the University of Bath evaluated the fatigue properties of wood laminates and a series of papers were published in JMS [68–71]. Initial work [68] was performed in flexure because turbine blades are effectively rotating beams subject to gravity and wind loads. The hardwood species selected was *Khaya ivorensis* (African mahogany) freely available in a 4-mm thick rotary-peeled veneer and commonly used for the manufacture of packing cases. Wood was laminated with a room temperature cure epoxy resin and cured in a vacuum bag. Solid Sitka spruce (*P. sitchensis*) softwood was also evaluated in fatigue in order to understand fatigue damage mechanisms. Wood samples were fatigued sinusoidally in four-point loading in a servo-hydraulic fatigue machine under load control at a constant rate of stress application and over a range of R ratios (minimum cyclic stress/maximum cyclic stress) from 0.5 to −1 (reversed loading). Stress versus log number of cycles to failure curves were linear and reversed loading resulted in the shortest fatigue lives, represented on a constant life diagram. Increased moisture content reduced fatigue life. Observations of the cellular structure of spruce, prepared by microtoming, following increasing numbers of fatigue cycles revealed

the formation of compression kinks in adjacent double cell walls which after further load cycles resulted in cell wall buckling, the formation of visible compression creases on the compression face of the wood beam and ultimately fracture.

Commercial turbine blades comprise essentially a leading edge D-spar with a foam trailing edge contained within an external FRP skin. Hence the blade faces at any point in their rotation see either a compressive or tensile load which can reverse during rotation. Attention therefore turned to fatigue of Khaya in compression, tension or reversed loading [69] using a much higher capacity 200 kN fatigue machine. Constant life lines were produced for a range of R ratios and compression fatigue was observed to be most damaging due to cell wall buckling. A size effect in fatigue was not observed, explained by the orthotropic nature of wood and insensitivity to the density of surface flaws.

Two papers followed on the fatigue properties of jointed wood laminates [70, 71] containing scarf joints which are a featured of laminated wood blades. The fatigue life of jointed Khaya, beech (*F. sylvatica*) and poplar (*Populus* sp.) were summarised in constant life diagrams from S–N data generated at $R = +3, -3, -1, -0.84$ and 0.33 together with static strengths in compression and tension (e.g. Fig. 10). Regression analysis was performed and 50% probability median regression 95% survival probability curves were presented. S–N data for the three wood species at $R = -1$ was normalised with respect to their compressive strengths and the S–N curves were found to coincide. It was proposed that simple triangulated constant life lines
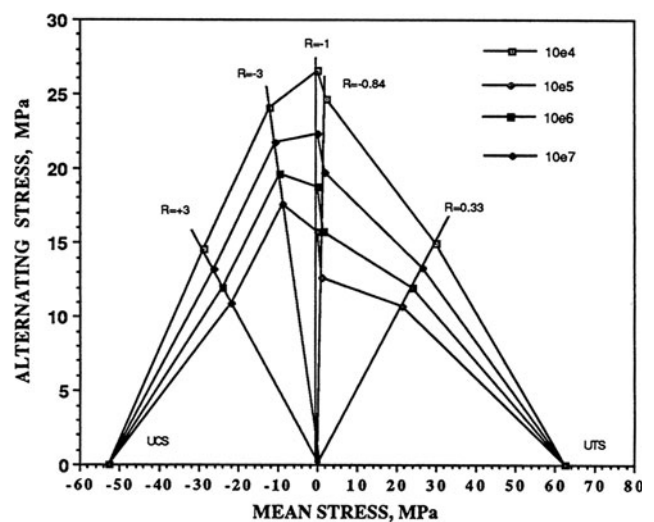
Fig. 10 Constant life diagram for scarf-jointed poplar derived from 50% probability mean regression curves for 10^4 (*upper* bound), 10^5, 10^6 and 10^7 (*lower* bound) cycles [70]

could be constructed from the static tensile and compressive strengths of wood species and S–N data for fatigue life in reverse loading [70]. Attention then turned to complex loading experienced by turbine blades, particularly when starting rotation and when shutting down under emergency conditions. A life prediction model was developed [71] for wood species based on $R = -1$ (reversed loading) fatigue data, tensile strength and compressive strength. Complex load–time histories derived from turbine blades fitted with data loggers was analysed using the rainflow method and the Palmgren–Miner damage summation rule. Scarf-jointed poplar was subjected to complex load–time histories and fatigue life was predicted via rainflow analysis applied to constant amplitude fatigue data and static properties. The predictive accuracy of the model was good in predominantly compressive loading and conservative in predominantly tensile loading.

The final paper on fatigue [72] concerns the evaluation of fatigue damage in relation to hysteresis in wood–epoxy laminates. In compression–compression fatigue under constant amplitude load control, hysteresis loops expand in size and loops shift along the compressive strain axis indicating compressive creep. The reverse occurs in tension–tension with tensile creep observed and some reduction in dynamic modulus. The two aspects of hysteresis development are captured in reverse loading (Fig. 11). Behaviour in the compressive quadrant is quite different to the tensile quadrant where there is a much bigger change in dynamic modulus with time. Dynamic modulus, loop area and minimum/maximum strains were plotted versus cycles summarising the accumulation of fatigue damage development. The laminated wood fatigue database and methods for life prediction in fatigue reported in JMS have subsequently been embodied in the design of commercial wind turbine blades.
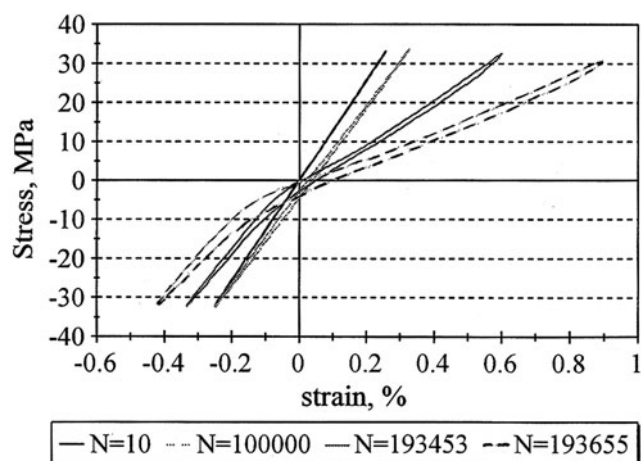
Fig. 11 Captured hysteresis loops for Khaya in reversed loading at $R = -1$ [72]

Conclusions

This review of JMS papers on wood has been restricted by the lack of reference to associated papers in other journals. However, the JMS papers contain a wealth of citations opening the door to a cornucopia of key literature references on wood. It is clear that since 1966 research on wood developed in phases as new experimental techniques became available, e.g. ion beam thinning, or commercial needs arose, e.g. the requirement for fatigue life data for wind turbine blades. Although wood as an engineering material has a pedigree going back for thousands of years there is still much to learn about its structure-related properties and papers on wood appearing in the pages of JMS continue to increase in number. In Part 2 of this review, the topics of wood modification, fire, carbonised wood and chars, wood–polymer composites and wood–cement composites will be examined from the JMS literature.

References

1. Dinwoodie JM (2000) Timber—its nature and behaviour. E & FN Spon, London, New York
2. Bodig J, Jayne BA (1982) Mechanics of wood and wood composites. Van Nostrand Reinhold, New York
3. Nakao S, Nakano T (2011) J Mater Sci 46:4748. doi:10.1007/s10853-011-5385-z
4. Entwistle KM, Terrill NJ (2000) J Mater Sci 35:1675. doi:10.1023/A:1004755913978
5. Entwistle KM, Navaranjan N (2001) J Mater Sci 36:3855. doi:10.1023/A:1017997516662
6. Entwistle KM, Navaranjan N (2001) J Mater Sci 37:539. doi:10.1007/s10853-006-1460-2
7. Entwistle KM, Kong K, MacDonald MA, Navaremjan N, Eichhorn SJ (2007) J Mater Sci 42:7263. doi:10.1007/s10853-006-1460-2
8. Färber J, Lichtenegger HC, Reiterer A, Stanzl-Tschegg S, Fratzl P (2000) J Mater Sci 36:5087. doi:10.1023/A:1012465005607
9. Ansell MP, Mwaikambo LY (2009) In: Eichhorn SJ, Hearle JWS, Jaffe M, Kikutani T (eds) Handbook of textile fibre structure, vol 2. Woodhead Publishing Limited, Oxford
10. Jang HF, Robertson AG, Seth RS (1992) J Mater Sci 27:6391. doi:10.1007/BF00576290
11. Fahlen J, Salmen L (2003) J Mater Sci 38:119. doi:10.1023/A:1021174118468
12. Navaranjan N, Blaikie RJ, Parbhu AN, Richardson JD, Dickson AR (2008) J Mater Sci 43:4323. doi:10.1007/s10853-008-2636-8
13. Reiterer A, Lichtenegger H, Fratzl P, Stanzl-Tschegg SE (2001) J Mater Sci 36:4681. doi:10.1023/A:1017906400924
14. Bergander A, Salmén L (2002) J Mater Sci 37:151. doi:10.1023/A:1013115925679
15. Hori R, Müller M, Watanabe U, Lichtenegger H, Fratzl P, Sugiyama J (2002) J Mater Sci 37:4279. doi:10.1023/A:1020688132345
16. Orso S, Wegst UGK, Arzt E (2006) J Mater Sci 41:5122. doi:10.1007/s10853-006-0072-1
17. Konnerth J, Gierlinger N, Keckes J, Gindl W (2009) J Mater Sci 44:4399. doi:10.1007/s10853-009-3665-7
18. Adsumalli RB, Mook WM, Passas R, Schwaller P, Michler J (2010) J Mater Sci 45:2558. doi:10.1007/s10853-010-4226-9

19. Xu P, Liu HW, Donaldson LA, Zhang Y (2011) J Mater Sci 46:534. doi:10.1007/s10853-010-5000-8
20. Bulota M, Jääskeläinen AS, Paltakari J, Hughes M (2011) J Mater Sci 46:3387. doi:10.1007/s10853-010-5227-4
21. Pierce CB, Dinwoodie JM (1977) J Mater Sci 12:1955. doi:10.1007/BF00561966
22. Hunt DG (1984) J Mater Sci 19:1456. doi:10.1007/BF00563040
23. Hunt DG (1986) J Mater Sci 21:2088. doi:10.1007/BF00547951
24. Hunt DG, Shelton CF (1987) J Mater Sci 22:313. doi:10.1007/BF01160586
25. Hunt DG (1990) J Mater Sci 25:3671. doi:10.1007/BF00575403
26. Entwistle KM, Zadoroshnyj A (2008) J Mater Sci 43:967. doi:10.1007/s10853-007-2138-0
27. Kelley SS, Rials TG, Glasser WG (1987) J Mater Sci 22:617. doi:10.1007/BF01160778
28. Kubat DG, Samuelsson S, Klason C (1989) J Mater Sci 24:3541. doi:10.1007/BF02385737
29. Kubat DG, Klason C (1991) J Mater Sci 26:5261. doi:10.1007/BF01143220
30. Ebrahimzadeh PR, Kubat DG (1993) J Mater Sci 28:5668. doi:10.1007/BF00367845
31. Ebrahimzadeh PR, McQueen DH (1998) J Mater Sci 33:1201. doi:10.1023/A:1004373525437
32. Eligon AM, Achong A, Saunders R (1992) J Mater Sci 27:3442. doi:10.1007/BF01151818
33. Wadso L (1994) J Mater Sci 29:2367. doi:10.1007/BF00363428
34. Furuta Y, Obata Y, Kanayama K (2001) J Mater Sci 36:887. doi:10.1023/A:1004838831791
35. Neagu RC, Gamstedt EK (2007) J Mater Sci 42:10254. doi:10.1007/s10853-006-1199-9
36. Placet V, Passard J, Perre P (2008) J Mater Sci 43:3210. doi:10.1007/s10853-008-2546-9
37. Arnold M (2010) J Mater Sci 45:669. doi:10.1007/s10853-009-3984-8
38. Lavers GM (1983) The strength properties of timber, BULLETIN 50, Forest Products Research Laboratory, 3rd edn, revised by Moore G. HMSO, London
39. US Forest Products Laboratory (1974) Wood handbook: wood as an engineering material. agriculture handbook no. 72. USDA, Madison
40. BS EN 1995–1-1 (2004) Eurocode 5: design of timber structures. General—Common rules and rules for buildings. British Standards Institute, London
41. Kahle E, Woodhouse J (1994) J Mater Sci 29:1250. doi:10.1007/BF00975072
42. Obataya E, Ono T, Norimoto M (2000) J Mater Sci 35:6317. doi:10.1023/A:1026795009861
43. Eichhorn SJ, Sirichaisit J, Young RJ (2001) J Mater Sci 36:3129. doi:10.1023/A:1017969916020
44. André N, Labbé N, Rials TG, Kelley SS (2006) J Mater Sci 41:1879. doi:10.1007/s10853-006-4433-6
45. Backman AC, Lindberg KAH (2001) J Mater Sci 36:3777. doi:10.1023/A:1017986119559
46. Birkinshaw C, Buggy M, Carew A (1989) J Mater Sci 24:359. doi:10.1007/BF00660981
47. Yamasaki M, Sasaki Y (2003) J Mater Sci 38:603. doi:10.1023/A:1021818513464
48. Katz JL, Spencer P, Wang Y, Misra A, Marangos O, Friis L (2008) J Mater Sci 43:139. doi:10.1007/s10853-007-2121-9
49. Ferguson WG, Yew FK (1977) J Mater Sci 12:264. doi:10.1007/BF00566266
50. Jeong GY, Hindman DP (2009) J Mater Sci 44:3824. doi:10.1007/s10853-009-3518-4
51. Jeong GY, Hindman DP, Zink-Sharp A (2010) J Mater Sci 45:5820. doi:10.1007/s10853-010-4658-2
52. Nadeau JS, Bennett R, Fuller ER (1982) J Mater Sci 17:2831. doi:10.1007/BF00644658
53. Boatright SWJ, Garrett GG (1983) J Mater Sci 18:2181. doi:10.1007/BF00555013
54. Bentur A, Mindess S (1986) J Mater Sci 21:559. doi:10.1007/BF01145523
55. Vautrin A, Harris B (1987) J Mater Sci 22:3707. doi:10.1007/BF01161482
56. Prokopski G (1993) J Mater Sci 28:5995. doi:10.1007/BF00365010
57. Prokopski G (1995) J Mater Sci 30:4745. doi:10.1007/BF01153088
58. Thuvander F, Jernkvist LO, Gunnars J (2000) J Mater Sci 35:6259. doi:10.1023/A:1026766203501
59. Thuvander F, Sjodahl M, Berglund LA (2000) J Mater Sci 35:6267. doi:10.1023/A:1026722521248
60. Thuvander F, Berglund LA (2000) J Mater Sci 35:6277. doi:10.1023/A:1026778622156
61. Tschegg EK, Reiterer A, Pleschberger T, Stanzl-tschegg SE (2001) J Mater Sci 36:3531. doi:10.1023/A:1017940903011
62. Reiterer A, Burgert I, Sinn G, Tschegg S (2002) J Mater Sci 37:935. doi:10.1023/A:1014339612423
63. Reiterer A, Tschegg S (2002) J Mater Sci 37:4487. doi:10.1023/A:1020610231862
64. Chen Z, Gabbitas B, Hunt D (2006) J Mater Sci 40:1929. doi:10.1007/s10853-005-1213-7
65. Chen Z, Gabbitas B, Hunt D (2006) J Mater Sci 41:3645. doi:10.1007/s10853-006-6292-6
66. Chen Z, Gabbitas B, Hunt D (2006) J Mater Sci 41:7247. doi:10.1007/s10853-006-0913-y
67. Gougeon M (2005) The Gougeon Brothers on boat construction, 5th edn. Gougeon Bros. Inc., Bay City
68. Tsai KT, Ansell MP (1990) J Mater Sci 25:865
69. Bonfield PW, Ansell MP (1991) J Mater Sci 26:4765. doi:10.1007/BF00612416
70. Bond IP, Ansell MP (1998) J Mater Sci 33:2751. doi:10.1023/A:1017565215274
71. Bond IP, Ansell MP (1998) J Mater Sci 33:4121. doi:10.1023/A:1004440801331
72. Hacker CL, Ansell MP (2001) J Mater Sci 36:609. doi:10.1023/A:1004812202540